

Distribution Agreement

In presenting this thesis as a partial fulfillment of the requirements for a degree from Emory University, I hereby grant to Emory University and its agents the non-exclusive license to archive, make accessible, and display my thesis in whole or in part in all forms of media, now or hereafter now, including display on the World Wide Web. I understand that I may select some access restrictions as part of the online submission of this thesis. I retain all ownership rights to the copyright of the thesis. I also retain the right to use in future works (such as articles or books) all or part of this thesis.

Catherine Urbano

March 30, 2018

The Development of Dual-Tropic CXCR4/CCR5 HIV-1 Entry Inhibitors

by

Catherine Urbano

Dr. Dennis Liotta
Adviser

Department of Chemistry

Dr. Dennis Liotta
Adviser

Dr. Jose Soria
Committee Member

Dr. Laura Otis
Committee Member

2018

The Development of Dual-Tropic CXCR4/CCR5 HIV-1 Entry Inhibitors

By

Catherine Urbano

Dr. Dennis Liotta

Adviser

An abstract of
a thesis submitted to the Faculty of Emory College of Arts and Sciences
of Emory University in partial fulfillment
of the requirements of the degree of
Bachelor of Arts with Honors

Department of Chemistry

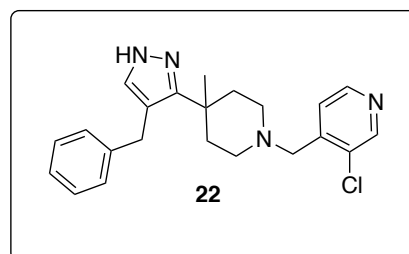
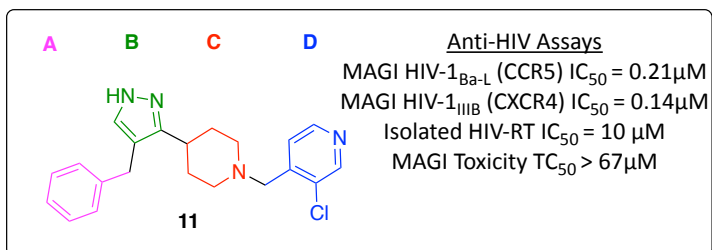
2018

Abstract

The Development of Dual-Tropic CXCR4/CCR5 HIV-1 Entry Inhibitors

By Catherine Urbano

The CDC estimates that 1.2 million Americans aged 13 years and older are living with HIV infection, however only 87% are diagnosed and only a shocking 36% are engaged in treatment. Despite 26+ HIV drug therapies on the market, drug resistance, affordability, and side effects are still major concerns. To combat these obstacles, our research specifically focused on designing a singular compound with dual CCR5 and CXCR4 activity. From prior work conducted in our lab, we identified a compound composed of a pyrazole-piperidine core that inhibited both receptors. After an extensive SAR study, compound **11** was identified as the lead target. In addition to containing dual-tropic activity, **11** also demonstrated an off-target effect against HIV reverse transcriptase. Saturated transfer difference NMR studies indicated that compound **22** would remove reverse transcriptase activity. Our efforts described herein focus on understanding the functional group tolerance of the A-ring, but also efforts toward eliminating reverse transcriptase activity via the synthesis of **22**.



The Development of Dual-Tropic CXCR4/CCR5 HIV-1 Entry Inhibitors

By

Catherine Urbano

Dr. Dennis Liotta

Adviser

A thesis submitted to the Faculty of Emory College of Arts and Sciences
of Emory University in partial fulfillment
of the requirements of the degree of
Bachelor of Arts with Honors

Department of Chemistry

2018

Acknowledgements

I would like to thank Dr. Liotta for providing me the opportunity to conduct research in his lab and for being a wonderful mentor and professor throughout my time at Emory. I would also like to thank Dr. Anthony Prosser and Dr. Michelle Kim for being patient, kind, and wise mentors. Michelle, you have taught me so much throughout the years and have motivated me to keep going despite countless failed reactions. I aspire to one day be as intelligent and kind as you.

I would like to thank Dr. Soria and Dr. Otis for being on my committee and for being wonderful professors. Your teaching styles have provoked me to approach problems in new ways and to think about concepts differently. I truly appreciate the time and effort you have invested in teaching me and serving on my committee.

Lastly, I would like to thank all my family, friends, and the rest of the Liotta lab for their support throughout this process.

Table of Contents

Introduction.....	1
Results.....	6
Identification of Lead Compound.....	6
Overview of SAR on A, B, C, and D-rings.....	8
Synthesis of Novel A-ring Derivatives	11
Synthesis of Methylated Derivative Compound 22	13
Conclusion.....	24
Experimentals.....	26
References.....	32

Figures, Tables, and Schemes Table of Contents

Figure 1. CDC Statistics of HIV in America.....	1
Figure 2. HIV Viral Entry Mechanism.....	3
Figure 3. Current Entry Inhibitor Chemical Structures.....	5
Figure 4. Virtual Screening Process and Identification of Scaffold.....	6
Figure 5. Anti-HIV profile of Compound 2	7
Table 1. SAR Study on A, B, C, and D-ring	10
Scheme 1. Synthetic Pathway of A-ring Derivatives.....	12
Table 2. Anti-HIV Activity for Novel A-ring Derivatives.....	13
Figure 6. Model Compound used in STD-NMR experiments.....	14
Figure 7. Overview of the STD-NMR experiment.....	15
Figure 8. STD-NMR results.....	16
Figure 9. Synthetic Target to Remove RT activity.....	16
Scheme 2. Proposed synthetic strategy for compound 22	17
Scheme 3. Unsuccessful Formation of Weinreb Amide.....	18
Scheme 4. Unsuccessful Addition of Grignard Reagent.....	18
Scheme 5. Unsuccessful Formylation/Cyclization Reaction.....	20
Scheme 6. Model Compound with Additional Methyl Group.....	20
Scheme 7. Nitrile Group Functionalization of alpha-Carbon.....	21
Scheme 8. Sonogashira Coupling/Cyclization of Final Product.....	22
Figure 10. Hypothesized Steric Hindrance of Additional Methyl Group.....	23
Scheme 9. Proposed Mechanism of Sonogashira coupling/cyclization.....	24

Introduction

The notion that HIV is a problem of the past or restricted to the developing world is far from the truth. In 2016, roughly 36.7 million people worldwide were infected with human immunodeficiency virus (HIV).¹ In the same year, there were 1.8 million newly infected individuals and 1 million deaths from AIDS-related illnesses. In the United States alone, 1.2 million Americans were infected with HIV in 2015 with nearly 50,000 Americans becoming newly infected each year. Despite initiatives to increase awareness, there were surprising still 13% of HIV-infected individuals who were unaware of their infection (Figure 1). Less than half of the individuals aware of their infection (39%) were actively seeing a doctor, and roughly 36% of diagnosed patients were actively engaged in Highly Active Anti-Retroviral Therapy (HAART).²

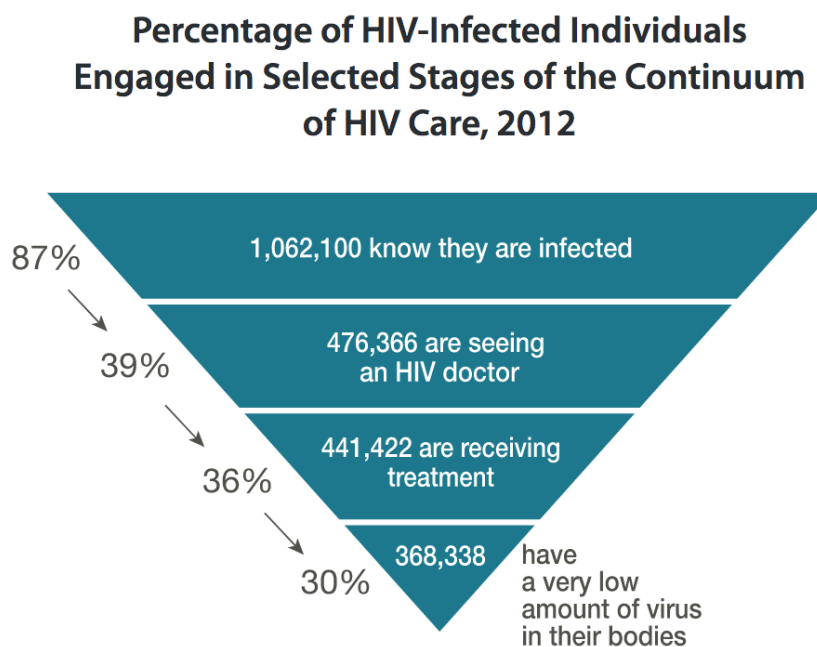


Figure 1. Percentage of HIV-Infected Americans aware of their illness and engaged in treatment as of 2012.²

HAART therapy is currently the gold standard of treatment involving a combination of at least three antiretroviral drugs that curbs viral replication to restore immune function³. These “drug cocktails” typically include non-nucleoside and nucleoside reverse transcriptase inhibitors (NNRTIs/NRTIs), integrase inhibitors, and protease inhibitors⁴. Once an inevitably fatal disease, HIV can now be managed by HAART into a chronic condition with a near normal life expectancy. The current regimen poses a significant financial burden and can cause the virus to become drug resistant. Patients on HAART have a higher potential for adverse drug-drug interactions as well as suffer from long term side effects making patient compliance challenging. Therefore, a single multi-targeting agent would be a more economically efficient treatment that could potentially circumvent issues associated with current HIV regimens.

The HIV virus gradually destroys the immune system. Viral particles target and destroy CD4+ T cells leaving the host susceptible to opportunistic infections which leads to AIDS (acquired immune deficiency syndrome). Infection begins when the virus binds to the T cell via interactions between viral envelope protein gp120 and glycoprotein CD4 on the T cell as shown in Figure 2. This binding interaction initiates a structural change within the virus that exposes the V3 loop, a chemokine binding region of gp120. Gp120 binds to one of two chemokine co-receptors, CCR5 or CXCR4, providing a stable two-pronged attachment of the virus to the host cell. The M-tropic strain of the virus gains entry into the cell via attachment to CCR5 (termed R5 viruses) while the more virulent T-tropic strain enters via attachment to CXCR4 (termed X4 viruses). In some cases, the virus presents itself as a mixed tropic strain using both CCR5 and CXCR4 (termed R5X4 viruses). The viral envelope subsequently fuses with the cell membrane

and injects the viral payload through the viral protein gp41. The virus is then able to hijack the host cell's cellular machinery, replicate itself, induce cellular apoptosis, and infect more cells⁵⁻⁶.

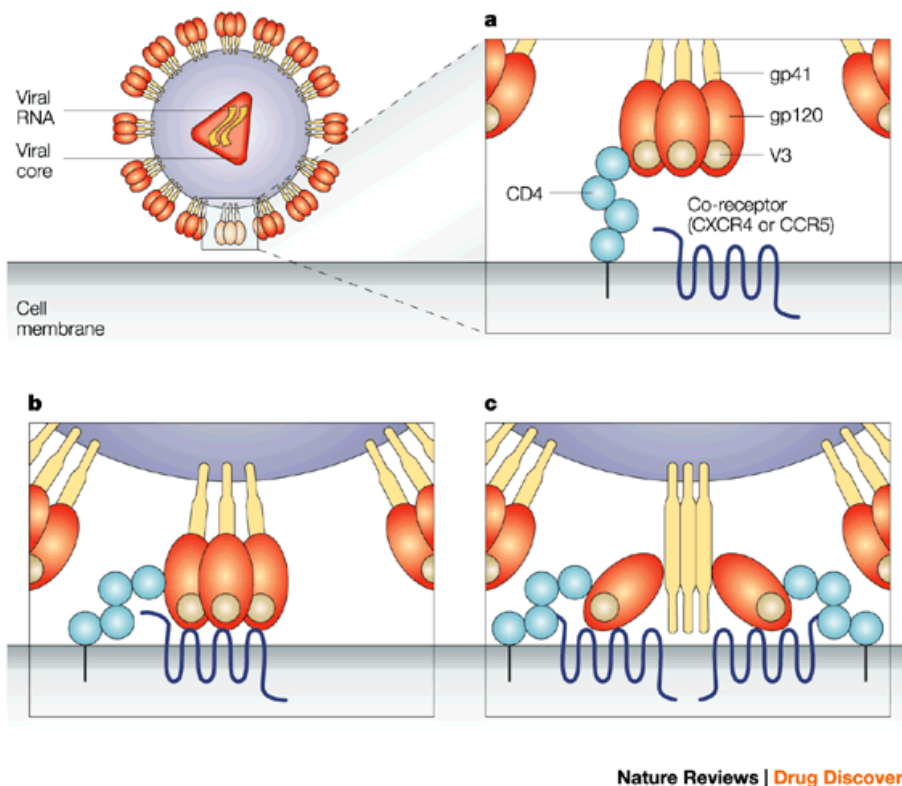


Figure 2. HIV viral entry mechanism⁷

Over two dozen FDA-approved drugs have been developed to target different stages of the HIV replication life cycle. However, only two of these FDA-approved drugs are entry inhibitors. Enfuvirtide (Fuzeon®), the first approved entry inhibitor, targets the viral protein gp41 which is responsible for viral fusion to the cellular membrane and injection of the viral load. Unfortunately, viral proteins quickly mutate and drug resistance rapidly emerges rendering the drug ineffective. The second entry inhibitor, maraviroc (Selzentry®), is a small molecule CCR5 receptor antagonist. Maraviroc is only prescribed for patients who have failed first and second-line treatments. Prior to prescription the patient must undergo an expensive

Trofile[®] screening to ensure they only carry the M-tropic strain. In an analysis of maraviroc treatment, 57% of patients who began treatment with predominately the M-tropic strain demonstrated a tropic shift to either the dual-tropic or T-tropic strain. It is evident that the selective pressure caused by maraviroc was extremely detrimental to patients as it facilitated the mutation of the virus to the more virulent strain and accelerated the progression of the disease⁸⁻⁹.

The inhibition of co-receptor CXCR4 has proven to be a more difficult target. To date, there are no FDA-approved drugs that inhibit CXCR4. A potent CXCR4 antagonist, bicyclam AMD3100 (Figure 3), entered clinical trials which were prematurely terminated due to elevated levels of hepato- and cardiotoxicity⁸. Another CXCR4 entry inhibitor, AMD11070, entered clinical trials, but trials were put on hold due to histologic changes to the liver observed in long-term animal studies. Interestingly, three of the four patients in trials demonstrated a tropism shift from dual/mixed tropic viruses to exclusively R5 virus by day 10. This study showed the possibility of an active CXCR4 antagonist used in the treatment of X4-tropic HIV-1.¹⁰

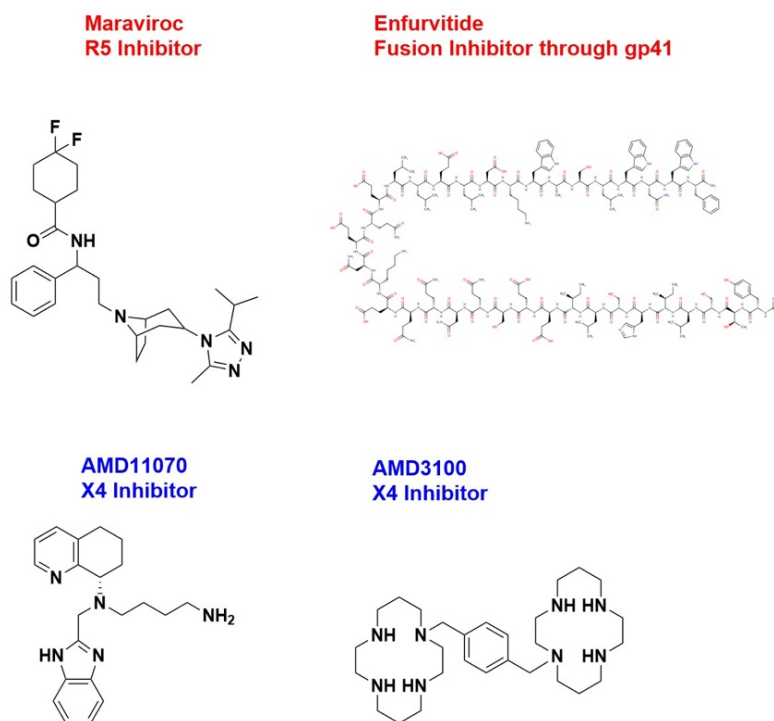


Figure 3. Current Entry Inhibitor Chemical Structures.

HIV treatments have certainly progressed in the last several decades but they still warrant improvements. Specifically, designing a single agent that simultaneously inhibits CCR5 and CXCR4 could combat issues such as drug resistance, drug-drug interaction, and long-term side effects associated with the chronic use of multiple drugs. Economically, a dual-tropic entry inhibitor would be more cost effective as it would eliminate the need for the expensive Trofile[®] test, and minimize the number of drugs taken in a single dose. In recent years, we have made efforts to design, synthesize, and optimize a dual-tropic chemokine inhibitor with a low toxicity profile. In the next section, I will discuss our recent progress towards this goal.

Results

Identification of Lead Compound

The first step in our research was to discover a compound that exhibited activity against CCR5 and CXCR4 receptors. Based on previous work that successfully created an automated design of ligands for multiple drug targets, we decided to use similar virtual screening techniques to identify potential CCR5/CXCR4 antagonists as shown in Figure 4¹¹. Bayesian statistical models were constructed for CCR5 and CXCR4 and trained with compounds known to be active or inactive¹². A virtual screen was conducted of compounds from the Aldrich Marketplace Select library (~5 million compounds) and ranked based on statistical activity. Of the top 300 compounds that exhibited activity, 14 compounds were purchased and tested. Anti-HIV activity was tested using CD4/CCR5/CXCR4 expressing MAGI cells (Multi-nuclear Activation of Galactosidase Indicator). Specifically, a MAGI HIV-1_{IIIB} assay was used to test CXCR4 activity and a MAGI HIV-1_{Ba-L} assay was used to test CCR5 activity. In addition, the compounds were tested against HIV-RT and assessed for toxicity.

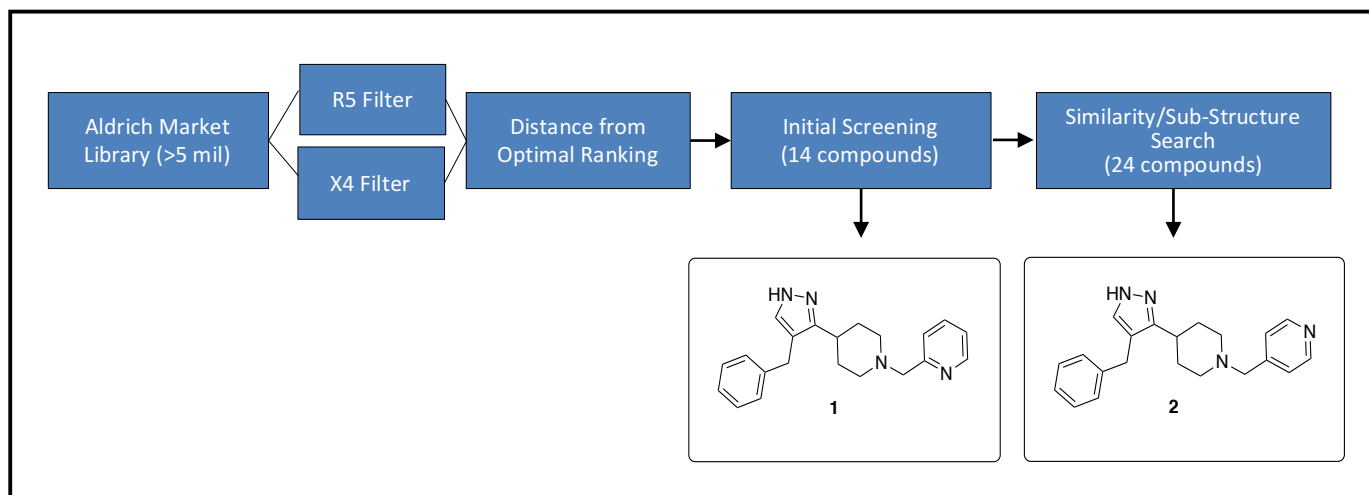


Figure 4. Virtual screening process and identification of scaffold. >5 million compounds were virtually screened for CCR5 and CXCR4 activity. Of the top 300 compounds, 14 were purchased and tested. Compound **1** demonstrated activity and proved to be synthetically accessible. 24 structurally similar compounds were purchased and tested. Compound **2** demonstrated the most potent dual-tropic activity.

Compound **1**, which consisted of a pyrazolo-piperidine core, demonstrated weak inhibition against CCR5- and CXCR4-utilizing HIV-1 strains and retained activity upon resynthesis. Twenty-four structurally similar compounds with pyrazolo-piperidine cores were purchased and subjected to a second round of testing. Eleven of the twenty-four compounds demonstrated activity against CCR5 and CXCR4. The most potent compound **2** consisted of a benzyl ring attached to the pyrazole and a 4-pyridal ring attached to the piperidine (Figure 5). It possessed an $IC_{50} = 3.8 \mu\text{M}$ and $0.8 \mu\text{M}$ activity against CCR5 and CXCR4, respectively, and displayed low levels of toxicity ($TC_{50} > 300 \mu\text{M}$). In addition, compound **2** possessed HIV-1 reverse transcriptase (RT) activity. In other words, the compound disrupted not only viral entry, but also intracellular viral replication. This unanticipated and undesirable off-target effect prompted us to remove RT activity.

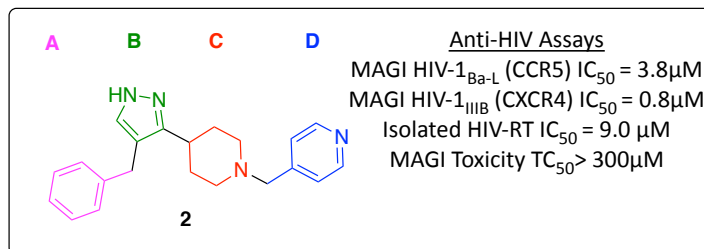


Figure 5. Anti-HIV profile of Compound **2**.

Though compound **2** demonstrated moderate activity, it was not nearly at a potency level that would reach FDA-approval. Therefore, our initial efforts were focused on improving potency while maintaining low levels of toxicity. A structure-activity relationship around each ring system of **2** was investigated and its results are discussed in the following section.

Overview of SAR on A, B, C, and D-rings

Compound **2** can be dissected into four separate ring systems (Figure 5). By manipulating each of the ring systems, we can begin to understand what functional groups are tolerated and necessary to improve the compound's overall potency while maintaining low toxicity. Dr. Anthony Prosser conducted SAR studies around the A, B, and C-ring using the same benzyl D-ring, exemplified by compound **3**, due to synthetic ease. A systematic SAR was conducted beginning with the A-ring. We found that replacement of the benzyl A-ring with a methyl group (compound **4**) or extension of the carbon linker to form phenethyl (compound **5**) resulted in a decrease in activity. The loss in activity of compound **5** suggested that the binding pocket did not have the spatial capacity to accommodate the enlargement. It also indicated that other stabilizing forces, such as pi-stacking interactions, were disrupted. SAR analysis of the B-ring demonstrated deletion of the pyrazole moiety resulted in a loss of CXCR4 activity while

maintaining moderate CCR5 activity (compound **6**). Replacement of the pyrazole with a carbonyl resulted in no measurable activity against both CCR5 and CXCR4 (compound **7**). Compound **8** explored a ring contraction of the C-ring from a piperidine to a pyrrolidine. No measurable activity of pyrrolidine **8** was observed. When the piperidine nitrogen was shifted to the 3-position, **9** was rendered inactive against CXCR4 and a large potency loss against CCR5 (~18 fold) was observed. Lastly, analysis of the D-ring was performed. A complete deletion of the D-ring resulted in a decrease in activity (compound **10**). Over 50 D-ring derivatives were synthesized in our lab (data not shown) and from it, compound **11**, a 3-chloropyridine D-ring was the most potent while maintaining moderate levels of toxicity. Compound **11** was examined in the reverse transcriptase assay and found to have an $IC_{50} = 10 \mu\text{M}$, which was similar to the activity of **2**. Later sections discuss efforts to remove RT activity.

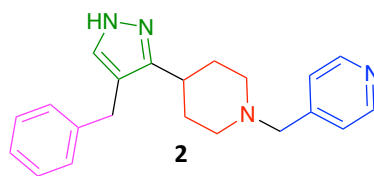


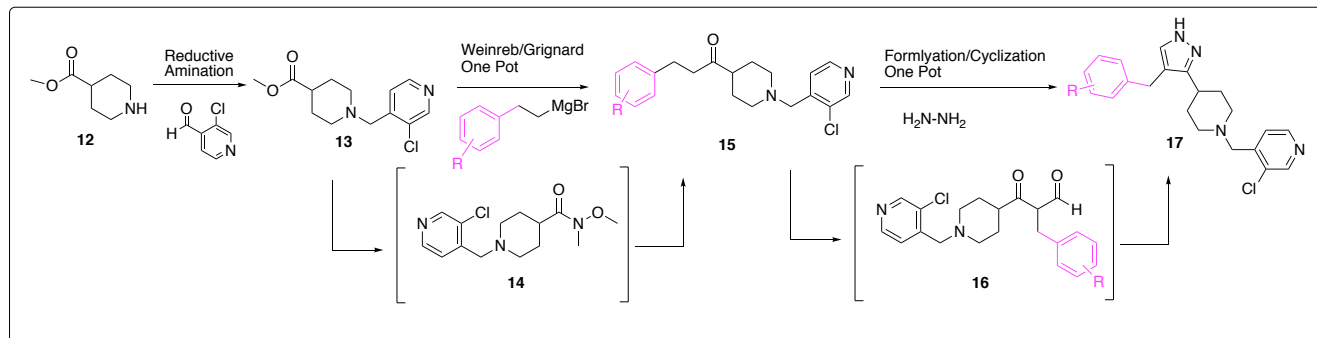
Table 1. Structure-Activity Relationship

Entry	Structure	MAGI Assay IC ₅₀ uM		TC ₅₀ uM
		CCR5	CXCR4	
3		18	13	>100
4		>300	>300	>300
5		>50	>50	>50
6		24	NA	125
7		>100	>100	>100
8		NA	NA	70
9		70	>100	>100
10		>100	>100	>100
11*		0.21	0.14	67

Table 1. SAR of A, B, C, and D-ring. Deletion of the A, B or D-ring or contraction of the C-ring results in a loss of activity. Compound **11** demonstrated the most potent dual-tropic activity.

Synthesis of novel A-ring Derivatives

A more comprehensive SAR analysis of the A-ring was further explored with the optimized D-ring. Synthesis began with commercially available methyl piperidine-4-carboxylate, **12**, which was the C-ring scaffold. The optimized D-ring was attached using a reductive amination reaction between the piperidine nitrogen and commercially available 3-chloroisonicotinaldehyde in the presence of sodium triacetoxyborohydride. The next step was to convert ester **13** into a Weinreb amide intermediate¹³ **14** with excess *N,O*-dimethylhydroxylamine hydrochloride at 0°C. An excess of the Grignard reagent with the desired A-ring was subsequently added to give ketone **15**. The ester was first transformed to the Weinreb amide before addition of the Grignard reagent to ensure mono-addition. This one-pot transformation of esters to analytically pure ketones gave rise to a straightforward synthetic pathway that allowed for easy A-ring modification. The last step was a one-pot formylation and cyclization reaction of **15** to the 1,3-dicarbonyl intermediate **16** using sodium hydride, 15-crown-5, and methyl formate. The cyclization reaction of **16** was achieved using hydrazine in the presence of methanol to form final product pyrazole **17**. Four novel compounds were synthesized through this 3-step sequence and their results are shown in Table 2.



Scheme 1. Synthetic pathway of A-ring derivatives

The MAGI assay results of compound **18** (where R1 = H) provided evidence that the elimination of the A-ring resulted in a loss of activity against CCR5 and CXCR4. This was consistent with the results observed with compound **4** (Table 1). With the cyclohexyl derivative **19**, a 10-fold decrease in potency was observed when compared to lead compound **11**. This suggested that an aromatic ring was not vital for activity. Contrary to our original hypothesis, it is possible that Van der Waals forces play a larger role in binding than pi-bond stacking. Replacement of the benzyl A-ring with *p*-fluoro benzene (compound **20**) also demonstrated a 10-fold decrease in potency, suggesting that a slightly deactivating group in the para position did not increase activity. The *p*-methyl **21** was also synthesized to investigate whether an additional methyl group in the para-position increases activity, but the compound has not been submitted for MAGI activity yet.

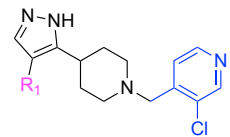


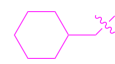
Table 2. Novel A-ring Derivatives				
Entry	R-group	MAGI Assay IC ₅₀ uM		TC ₅₀ uM
		CCR5	CXCR4	
11		0.21	0.14	67
18	H	NA	NA	>100
19		2.77	4.84	16.7
20		3.19	7.20	>30
21		To be Submitted		

Table 2. Anti-HIV activity for novel A-ring derivatives

The synthesis of these novel compounds shed some insight into the inhibition activity of our pyrazole-piperidine scaffold. The data suggested that complete or partial elimination of the A-ring resulted in a loss of activity against both chemokine co-receptors, but an aromatic A-ring was not essential for activity. MAGI data from **20** suggested that a small, slightly deactivating group in the para position did not improve potency. Despite these findings, the novel compounds did not demonstrate higher activity than our lead, **11** and therefore, the benzyl group is currently the most potent A-ring.

Synthesis of Methylated Derivative **22**

Initial anti-HIV testing of the dual-tropic series resulted in activity against both chemokine co-receptors, but also against reverse transcriptase (RT). This unexpected off-target effect seemed fortuitous at first, but optimizing the structure and activity against three targets

is monumentally challenging. It would also be difficult to decipher how much each target was truly responsible for anti-HIV activity. Because this task would be extremely difficult to accomplish, we focused our efforts on eliminating RT activity while maintaining CCR5 and CXCR4 activity. In order to do so, Dr. Cox performed a series of saturation transfer difference NMR (STD-NMR) experiments on a model compound **1** (Figure 6) to gain insight into which areas of the molecule were important for activity against each target.

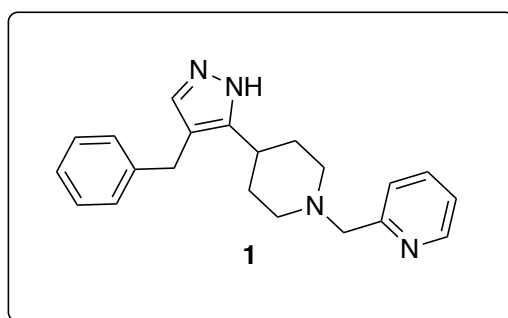


Figure 6. Model compound used in STD-NMR experiments.

STD-NMR is a ligand-based approach to determine protein-ligand interactions, and relies on the on/off exchange of the ligand in the receptor. An STD-NMR experiment takes the off-resonance spectrum (spectrum of ligand without irradiating the protein) with an on-resonance spectrum (spectrum with selective irradiation of the protein) as shown in Figure 7. The difference between the two spectra and the intensity of the peaks determines which hydrogen atoms are bound closely in the receptor. Only areas bound to the receptor will receive a transfer of signal that can be seen in the difference spectrum.

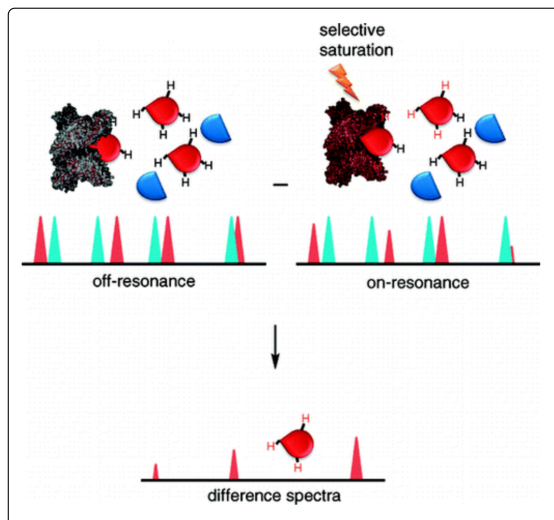


Figure 7. Overview of the STD-NMR experiment. The difference between the on-resonance and off-resonance spectrum determines which hydrogens are bound closely to the receptor¹⁴.

The STD-NMR results are highlighted in Figure 8 below. In Figure 8a, the results between **1** and CCR5 receptor suggested that the benzyl A-ring and the pyrazole B-ring were bound to the receptor in the major binding pocket as shown by the darker colored circles which indicate direct binding to the receptor. These results suggest that the piperidine C-ring and D-ring are solvent exposed and less crucial for binding (Figure 8a).

The NMR results for CXCR4 were similar to the results for CCR5. It suggested that the flanking A and D aromatic rings were critical for activity, and the benzyl A-ring and pyrazole B-ring were bound to the protein in the major pocket. Half of the piperidine C-ring is thought to be buried within the protein while the other half is solvent exposed. The 2-pyridyl D-ring was found to bind in the minor sub pocket through pi-stacking and hydrophobic interactions. (Figure 8b). The results of the STD-NMR experiments of HIV RT suggested that the piperidine-pyrazole B,C-ring core were primarily bound within the RT receptor (Figure 8c). Results indicated that the

piperidine C-ring is surrounded by hydrophobic residues and the pyrazole B-ring acts as a hydrogen donor to Val 179 (data not shown).

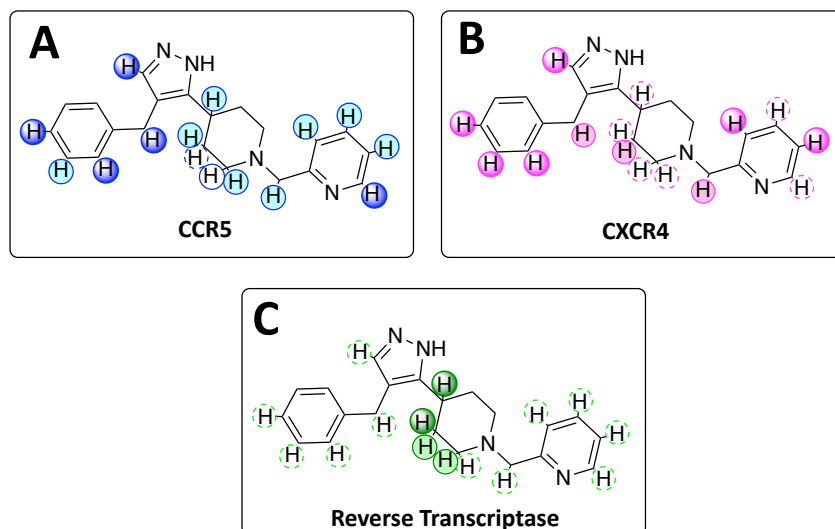


Figure 8. STD-NMR results. Darker circles correspond to more intense STD signals and therefore, areas more crucial to target binding.

Gratifyingly, the experiment suggested that the C-ring of **1** was mainly inside the RT binding pocket, which we were quick to exploit (Figure 8c). We hypothesized that a methyl group between the pyrazole and the piperidine ring system would disrupt binding to RT. According to the STD-NMR results, the C-ring area of the molecule was not crucial for CCR5/CXCR4 binding and we expect the methyl group to have no effect on dual-tropic activity. We set out to validate our hypothesis by synthesizing compound **22** (Figure 9).

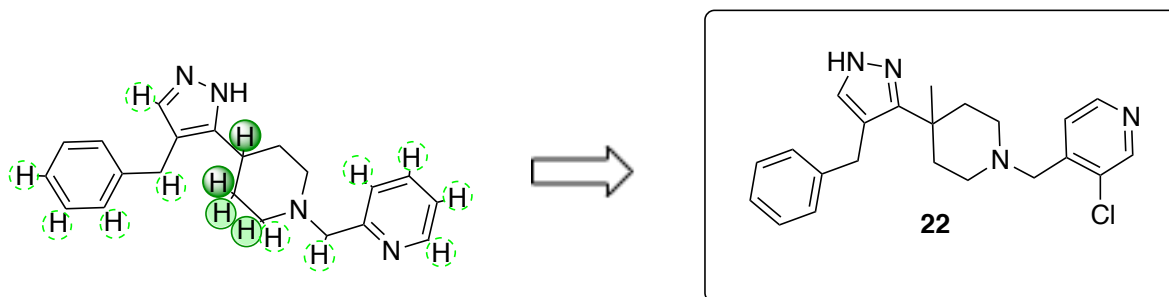
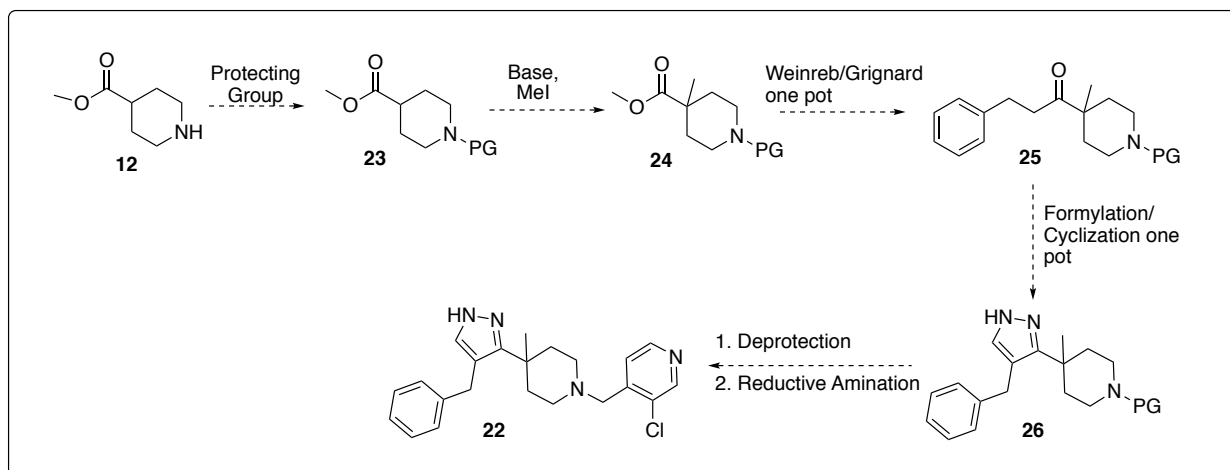


Figure 9. Synthetic target based on STD-NMR results to remove reverse transcriptase activity.

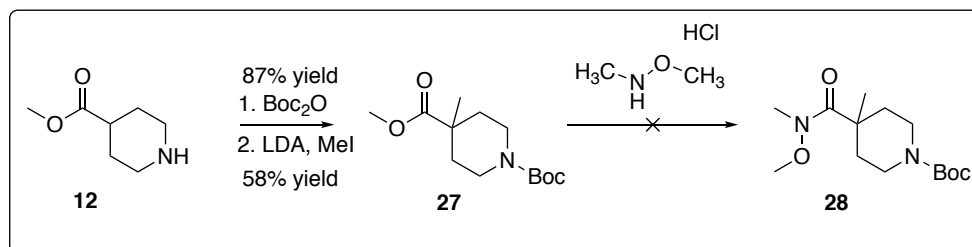
The proposed synthetic strategy for the synthesis of **22** was derived from the established route of the desmethyl parent compound **11** (Scheme 2). Beginning with commercially available methyl piperidine-4-carboxylate **12**, we planned to protect the piperidine nitrogen. The compound was to be methylated using a base and excess MeI to form compound **24**. A one pot Weinreb/Grignard reaction would convert methyl ester **23** to ketone **25**. A one pot formylation/cyclization reaction would be used to cyclize the B-ring and form compound **26**. Synthesis could be completed with a deprotection reaction followed by a reductive amination reaction to afford compound **22**.



Scheme 2. Proposed synthetic strategy for compound **22**.

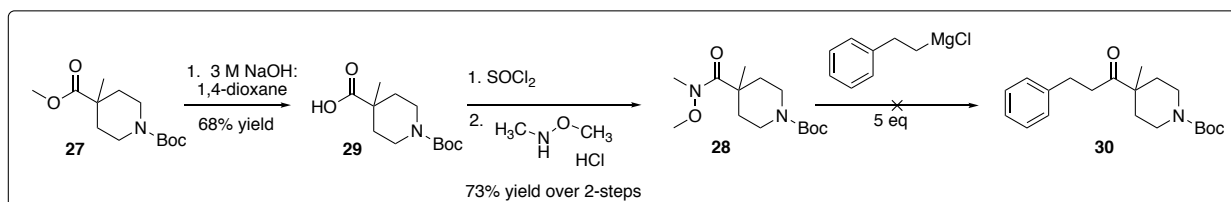
The 6-step proposed synthesis of methylated derivative **22** proved to be far more challenging than anticipated. Initial efforts began with tert-butyloxycarbonyl (boc) as the protecting group. Boc-protection of the piperidine nitrogen was achieved using boc anhydride and triethylamine. Next, the boc-protected intermediate was treated with freshly prepared lithium diisopropylamide (LDA) and excess methyl iodide (MeI) to form **27**. In the established route by Prosser et al.¹³, the methyl ester of **27** was converted to the Weinreb amide using *N,O*-

dimethylhydroxylamine in the presence of acid to prevent over addition during Grignard addition. But all efforts to attain Weinreb amide **28** were unsuccessful.



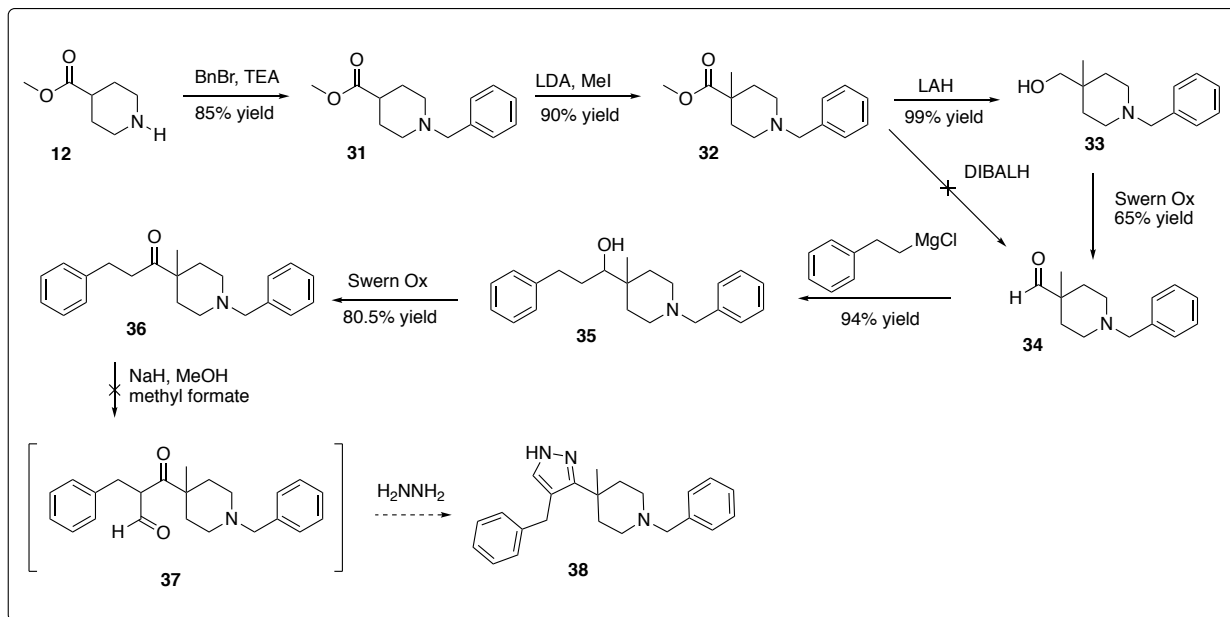
Scheme 3. Unsuccessful formation of Weinreb Amide.

Steric hindrance around the newly formed methyl group of **27** was suspected for reducing the reactivity of the methyl ester. Therefore, a nucleophilic acyl substitution reaction was explored to synthesize Weinreb amide **28**. The methyl ester **27** was transformed to the more reactive acyl chloride functional group as shown in Scheme 4. The methyl ester **27** was hydrolyzed to the free acid using sodium hydroxide in dioxane to form carboxylic acid **29**. The carboxylic acid **29** was converted into the acid chloride with thionyl chloride. The acid chloride successfully formed the Weinreb amide **28**. The next step was conversion of the Weinreb amide into ketone **30** using phenethylmagnesium chloride. Unfortunately, addition of the Grignard reagent did not result in any anticipated product.



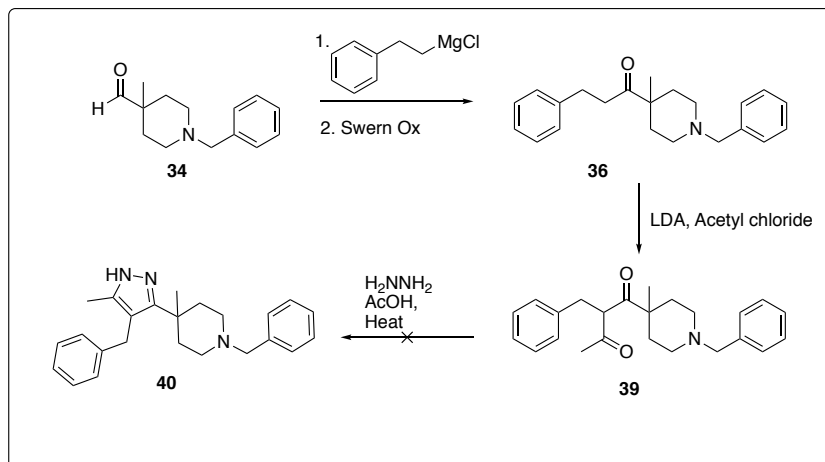
Scheme 4. Synthetic pathway via acyl chloride. Conversion of the carboxylic acid **29** to Weinreb Amide **28** via acyl chloride formation was successful, but subsequent Grignard addition was unsuccessful.

After several unsuccessful attempts to convert the Weinreb amide into ketone **30**, we hypothesized that converting the methyl ester to the more reactive aldehyde would make it more susceptible to nucleophilic attack. Beginning with methyl ester **12**, the piperidine nitrogen was benzyl protected to provide better UV-visibility. The methylation reaction using LDA and MeI yielded **32**. Efforts to directly convert methyl ester **32** with diisobutylaluminium hydride did not proceed to the desired aldehyde **34**. Consequently, we reduced **32** to alcohol **33** with lithium aluminum hydride (LAH). Several oxidation reactions were attempted with alcohol **33**. Oxidation of alcohol **33** was achieved with DMP, but purification of the byproducts led to low yields. A Parikh-Doering reaction did not yield any isolable aldehyde **34**. The Swern oxidation yielded the best results and the highest yield for aldehyde **34**. The Grignard addition of **34** with phenethylmagnesium chloride afforded compound **35**. The resulting secondary alcohol of **35** was then oxidized to **36** with the Swern oxidation. The next step was a one-pot formylation/cyclization reaction via formyl intermediate **37**. The formylation reaction did not proceed using the standard conditions with sodium hydride, methyl formate, and 15-crown-5 ether. Attempts to form sodium methoxide using sodium metal in methanol proved unsuccessful.



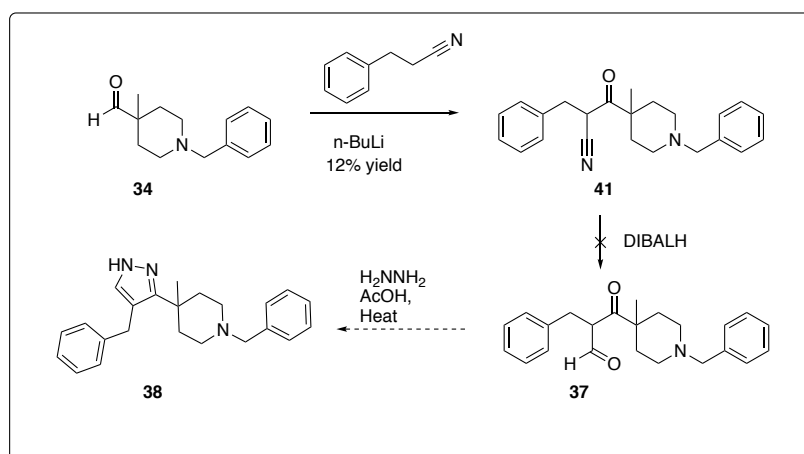
Scheme 5. Benzyl-protected synthetic pathway. Ketone **36** was not successfully converted to intermediate **37** or pyrazole **38**.

Our concern that the ketone could not be functionalized with the formyl group grew. Therefore, a model system was utilized to explore the synthetic pathway. Using acetyl chloride rather than methyl formate allowed us to explore stronger bases such as LDA . The ketone **36** was treated with LDA and acetyl chloride to furnish **39**. Although this was successful, the following cyclization step with hydrazine monohydrate, acetic acid and heat did not proceed to **40**. Despite varying conditions, only starting material was observed.



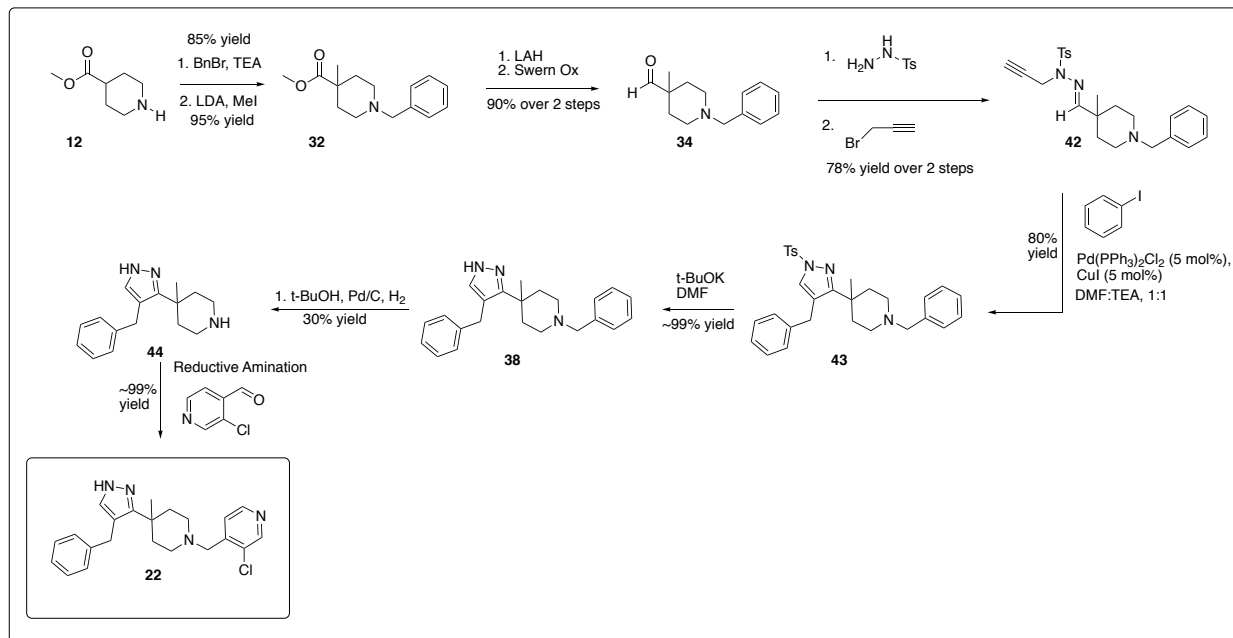
Scheme 6. Model compound with additional methyl group.

Though the cyclization of the acetyl group to the pyrazole was unsuccessful, it proved the capability to synthesize a dicarbonyl intermediate. We decided to attempt a nucleophilic substitution between aldehyde **34** and hydrocinnamitrile with hopes of reducing the resulting β-keto nitrile **41** intermediate into the aldehyde. The deprotonation of the hydrocinnamitrile was readily achieved with *n*-BuLi and condensed with aldehyde **34** to yield **41**. The reduction of the nitrile **41** into the aldehyde using DIBAL-H did not proceed and only starting material remained.



Scheme 7. Nitrile group functionalization of alpha-carbon.

We focused our efforts on a third synthetic strategy utilizing a Sonogashira coupling and cascade cyclization reaction to synthesize the pyrazole core¹⁵. Compound **12** was readily converted to aldehyde **34** and then the aldehyde was cleanly converted to the tosylhydrazone with *p*-TsCl. A substitution reaction of the tosylhydrazone intermediate with propargyl bromide formed compound **42**. A Sonogashira coupling reaction of **42** and iodobenzene yielded an intermediate which readily underwent a cascade reaction in the presence of triethylamine. The reaction simultaneously cyclized the pyrazole B-ring and attached the A-ring to afford compound **43**. A detosylation reaction of **43** was achieved using potassium tert-butoxide in DMF to provide the free pyrazole **38**. Pyrazole **38** was then subjected to a hydrogenation reaction to remove the benzyl protecting group yielding **44**. It is important to note here that *t*-BuOH was the solvent of choice as prior studies (unpublished) showed that methanol and ethanol led to alkyl addition onto the piperidine nitrogen. Lastly, a reductive amination reaction of **44** with 3-chloroisonicotinaldehyde led to final product **22**. Final product **22** was successfully synthesized. Overall, compound **22** took 9-steps to synthesize with a total yield of 13%.



Scheme 8. Sonogashira coupling and cascade cyclization of final product.

The unanticipated difficulties of synthesizing this molecule indicated that the additional methyl group altered the reactivity of the piperidine molecule. It was hypothesized that the addition of the methyl group sterically hindered the carbonyl carbon, reducing the susceptibility for nucleophilic attack (Figure 10).

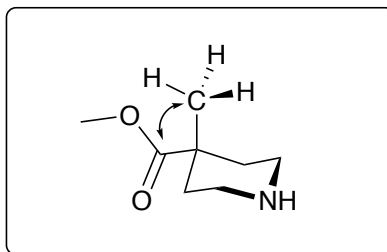
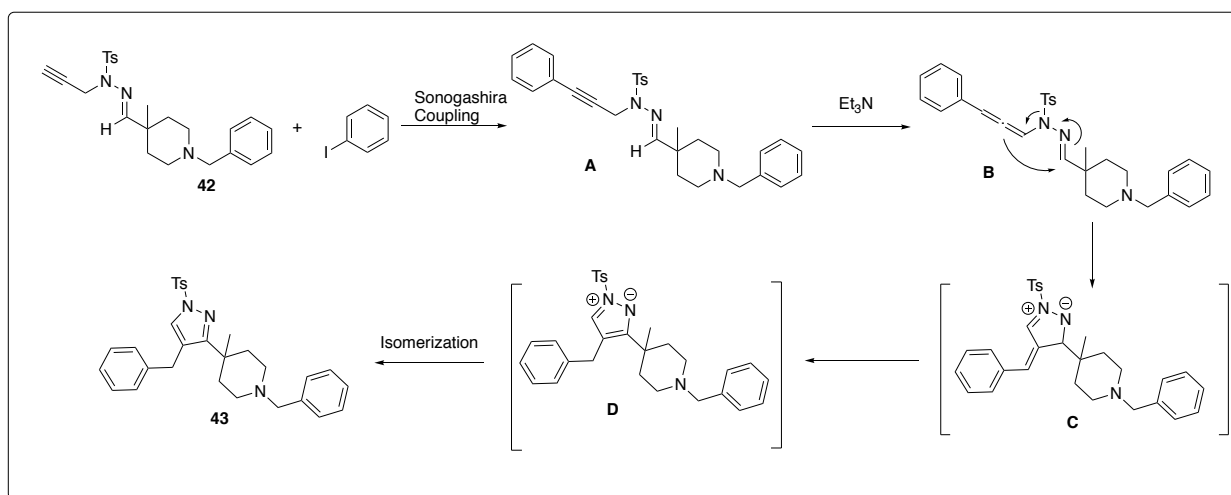


Figure 10. Hypothesized steric hindrance of additional methyl group.

The Sonogashira reaction was successful because the imine carbonyl was less sterically encumbered than the methyl ester moiety, and intermediate **A** was positioned for the intermolecular cyclization reaction. The proposed mechanism of the tosylhydrazone

intermediate **42** to the pyrazole **38** can be seen in Scheme 9. Compound **42** first undergoes a Sonogashira coupling of iodobenzene and *N*-propargyl sulfonylhydrazone. Triethylamine is used to facilitate the isomerization of compound **A** to allenic compound **B**. A spontaneous cyclization cascade reaction of intermediate **B** forms the pyrazole **C**. The isomerization of intermediate **C** and **D** give rise to the product **43**¹⁵.



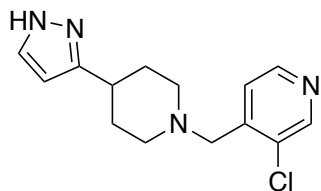
Scheme 9. Proposed mechanism of Sonogashira coupling and cascade cyclization reaction.

Conclusion

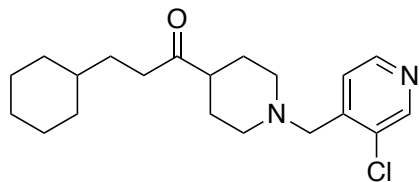
We have made significant progress in the development of a dual-tropic HIV chemokine co-receptor inhibitor. Virtual screening of the Aldrich Marketplace Select library and the resynthesis of key compounds led to the identification of a pyrazole-piperidine scaffold. Initial anti-HIV testing of our scaffold showed that it possessed activity against CCR5 and CXCR4 and also HIV RT activity. An SAR study of the A, B, C, and D-ring resulted in a lead compound **11**. Saturation difference NMR experiments of compound **1** were conducted in an effort to remove the RT activity. The NMR experiments showed that the addition of a methyl group on the piperidine ring would theoretically disrupt interactions between the compound and the RT

binding site while maintaining CCR5 and CXCR4 activity. The synthesis of the methylated compound **22** was achieved in 9-steps with an overall yield of 13%. The compound is currently out for testing. Future efforts will be focused on optimizing potency, maintaining a low toxicity profile, and removing RT activity to bring us closer to a dual-tropic HIV chemokine co-receptor inhibitor.

Experimentals

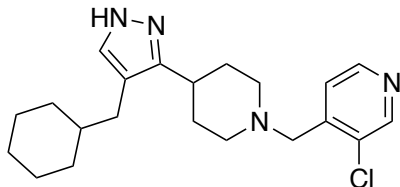


4-((4-(1H-pyrazol-5-yl)piperidin-1-yl)methyl)-3-chloropyridine (18). To a solution of 1-(1-((3-chloropyridin-4-yl)methyl)piperidin-4-yl)ethanone (1.20 g, 4.75 mmol) in THF (47.5 mL, 0.1 M) in a flame dried 100 mL round bottom flask was added NaH (60% wt, 0.855 g, 3.41 mmol, 4.50 eq) and stirred at room temperature. Methyl formate (7.32 mL, 119 mmol, 25 eq) was then added followed by 15-crown-5 (0.157 g, 0.712 mmol, 0.15 eq) and two drops of dry methanol. The reaction was tracked by LCMS and was quenched after 1 hr with 3 mL of dry methanol dropwise. The reaction was then diluted with hydrazine hydrate (0.252 mL, 4.75 mmol, 1 eq). Then the reaction was diluted with pure hydrazine (0.252 mL, 4.75 mmol, 1 eq). After an hour, the reaction was evaporated and then partitioned between water and EtOAc, and then basified with 10% NaOH solution. The layers were separated and the aqueous layer was extracted with DCM (3 times). The organic layers were combined, dried over anhydrous sodium sulfate, filtered, and concentrated. The crude mixture was then purified on a 2.4 gram combiflash column with a gradient from 0-70% DCM:MeOH:NH₄OH (9:1:0.1) in DCM to afford 4-((4-(1H-pyrazol-5-yl)piperidin-1-yl)methyl)-3-chloropyridine (0.75 g, 57% yield). ¹H NMR (400 MHz, CDCl₃) δ 8.51 (s, 1H), 8.43 (d, 5.2 Hz, 1H), 7.50 (s, 1H), 7.49 (s, 1H), 6.11 (d, *J* = 2.0 Hz, 1H), 3.62 (s, 2H), 2.97 (dt, *J* = 12, 4.8 Hz, 2H) 2.37 (ttt, *J* = 12, 4.0 Hz, 1H), 2.25 (t, *J* = 12 Hz, 2H), 1.98 (d, *J* = 14 Hz, 2H), 1.85 (m, 2H). ¹³C NMR (101 MHz, CDCl₃) δ 152.3, 149.1, 147.6, 145.5, 133.8, 1371.8, 124.3, 101.9, 58.5, 53.9, 53.4, 34.3, 32.2. LCMS 75-95% 3 minutes MeOH:H₂O gradient >95% pure rt = 0.644 min. LCMS 50-95% 8 minutes MeOH:H₂O gradient >95% pure rt = 0.826 min. HRMS calc'd for C₁₄H₁₈ClN₄ 277.1220; found [M+H] 277.1212.

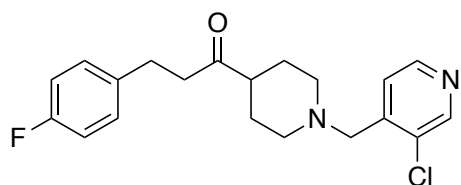


1-(1-((3-chloropyridin-4-yl)methyl)piperidin-4-yl)-3-cyclohexylpropan-1-one. A solution of methyl 1-((3-chloropyridin-4-yl)methyl)piperidine-4-carboxylate in THF (36.8 mL, 0.1 M) was added to a flame dried 100 mL round bottom flask containing *N,O*-dimethylhydroxylamine hydrochloride (0.431 g, 4.42 mmol, 1.2 eq) and stirred at 0°C. (2-cyclohexylethyl)magnesium bromide (18.42 mL, 18.41 mmol, 4.5 eq) was then added dropwise and the reaction was allowed to stir. The reaction was heated at room temperature and was allowed to stir until complete conversion to the ketone was observed by LCMS. The reaction mixture was quenched with a solution of saturated NH₄Cl slowly and allowed to stir for 10 minutes, then basified with 10% NaOH dropwise. The mixture was further partitioned with EtOAc and separated. The aqueous layer was extracted with EtOAc once more and then DCM twice. The organic layers were combined, dried over anhydrous sodium sulfate, filtered, and concentrated to afford 1-(1-

((3-chloropyridin-4-yl)methyl) piperidin-4-yl)-3-cyclohexylpropan-1-one (0.745 g, 57.9% yield). LCMS 75-95% 3 minutes MeOH:H₂O gradient >95% pure rt = 1.46 min; LCMS 50-95% 8 minutes MeOH:H₂O gradient >95% pure rt = 4.19 min. HRMS calc'd for C₂₀H₃₀ClN₂O 349.2047; found [M+H] 349.2035.

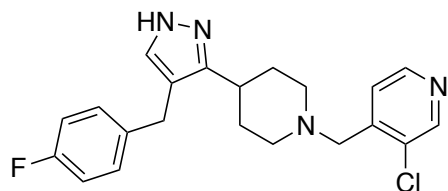


3-chloro-4-((4-(4-(cyclohexylmethyl)-1H-pyrazol-3-yl)piperidin-1-yl)methyl)pyridine (19). To a solution of 1-(1-((3-chloropyridin-4-yl)-3-cyclohexylpropan-1-one (0.7447 g, 2.135 mmol) in THF (21.34 mL, 0.1M) in a flame dried 100 mL round bottom flask was added NaH (60%wt, 0.384 g, 9.6 mmol, 4.5 eq) and stirred at RT. Methyl formate (2.56 g, 42.7 mmol, 20 eq) was then added followed by 15-crown-5 (0.071 g, 0.320 mmol, 0.15 eq). The reaction was tracked by LCMS and after 1 hour was quenched with 5 mL of H₂O dropwise. The reaction was then diluted with pure hydrazine (0.335 mL, 10.67 mmol, 5 eq) and a drop of methanol. The reaction was tracked by LCMS and an additional amount of NaH was added (60%wt, 0.171 g, 4.27 mmol, 2 eq). The next morning, the reaction was partitioned between water and EtOAc, and then basified with 10% NaOH solution. The layers were separated and the aqueous layer was extracted with DCM (3 times). The organic layers were combined, dried over anhydrous sodium sulfate, filtered, and concentrated. The crude mixture was then purified on a 2.4 gram combiflash column with a gradient from 0-70% DCM:MeOH:NH₄OH (9:1:0.1) in DCM to afford 3-chloro-4-((4-(4-(cyclohexylmethyl)-1H-pyrazol-3-yl)piperidine (57.2 mg, 7.0% yield). LCMS 75-95% 3 minutes MeOH:H₂O gradient >95% pure rt = 0.778. LCMS 50-95% 8 minutes MeOH:H₂O gradient >95% pure rt = 4.002. HRMS calc'd for C₂₁H₃₀ClN₄ 373.2159 found [M+H] 373.2151.

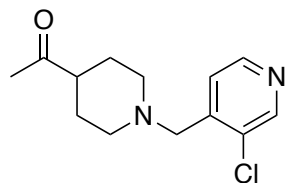


1-(1-((3-chloropyridin-4-yl)methyl)piperidin-4-yl)-3-(4-fluorophenyl)propan-1-one. A solution of 1-((3-chloropyridin-4-yl)methyl)-N-methoxy-N-methylpiperidine-4-carboxamide (1.0 g, 3.36 mmol) in THF (33.6 mL, 0.1 M) was added (4-fluorophenethyl)magnesium bromide (5.04 mL, 5.04 mmol, 1.5 eq) dropwise and the reaction was allowed to stir at 0°C. The reaction was heated to room temperature and tracked by LCMS. The remainder of (4-fluorophenethyl)magnesium bromide (19.59 mL, 19.59 mmol, 5.83 eq) was added dropwise and was allowed to stir at 0°C. The reaction was heated to room temperature and was allowed to stir until complete conversion to ketone was observed by LCMS. The reaction mixture was quenched with a solution of saturated NH₄Cl slowly and allowed to stir for 10 minutes, then basified with 10% NaOH dropwise. The mixture was further partitioned with EtOAc and separated. The aqueous layer was extracted with EtOAc once more and then DCM twice. The

organic layers were combined, dried over anhydrous sodium sulfate, filtered, and concentrated. The crude mixture was then purified on an 44 gram combiflash column with a gradient from 0-20% DCM:MeOH:NH₄OH (9:1:0.1) in DCM to afford 1-(1-((3-chloropyridin-4-yl) methyl) piperidin-4-yl)-3-(4-fluorophenyl)propan-1-one (0.274 g, 22.5% yield). LCMS 75-95% 3 minutes MeOH:H₂O gradient >95% pure rt = 0.862 min. LCMS 50-95% 8 minutes MeOH:H₂O gradient >95% pure rt = 3.36 min. HRMS calc'd for C₂₀H₂₃ClFN₂O 361.1483; found [M+H] 361.1478.

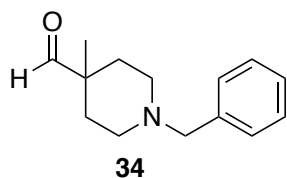


3-chloro-4-((4-(4-(4-fluorobenzyl)-4H-pyrazol-3-yl)piperidin-1-yl)methyl)pyridine (20). To a solution of 1-(1-((3-chloropyridin-4-yl) methyl) piperidin-4-yl)-3-(4-fluorophenyl)propan-1-one (0.274 g, 0.758 mmol) in THF (7.58 mL, 0.1 M) in a flame dried 100 mL round bottom flask was added NaH (60%wt, 0.136 g, 3.41 mmol, 4.5 eq) and stirred at RT. Methyl formate (0.91 g, 15.2 mmol, 20 eq) was then added followed by 15-crown-5 (0.025 g, 0.114 mmol, 0.15 eq) and two drops of dry methanol. The reaction was tracked by LCMS and after 1 hr was quenched with 3 mL of dry methanol dropwise. The reaction was then diluted with pure hydrazine (0.12 mL, 3.79 mmol, 5 eq). After the reaction was then diluted with hydrazine monohydrate (0.12 mL, 3.79 mmol, 5 eq). After an hour, the solvent was evaporated and the residue was partitioned between water and EtOAc, and then basified with 10% NaOH solution. The layers were separated and the aqueous layer was extracted with DCM (3 times). The organic layers were combined, dried over anhydrous sodium sulfate, filtered, and concentrated. The crude mixture was then purified on a 2.4 gram combiflash column with a gradient from 0-70% DCM:MeOH:NH₄OH (9:1:0.1) in DCM to afford 3-chloro-4-((4-(4-(4-fluorobenzyl)-1H-pyrazol-3-yl)piperidin-1-yl)methyl)pyridine (0.0572 g, 7.0 % yield). LCMS 75-95% 3 minutes MeOH:H₂O gradient >95% pure rt = 0.780 min. LCMS 50-95% 8 minutes MeOH:H₂O gradient >95% pure rt = 3.398 min. HRMS calc'd for C₂₁H₂₃ClFN₄ 385.1595; found [M+H] 385.1589

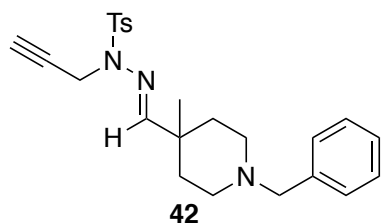


1-(1-((3-chloropyridin-4-yl) methyl) piperidin-4-yl)ethanone. A solution of methyl 1-((3-chloropyridin-4-yl)methyl)piperidine-4-carboxylate (1.2 g, 4.47 mmol) in THF (44.7 mL, 0.1 M) was added to a flame dried 100 mL round bottom flask containing *N,O*-dimethylhydroxylamine hydrochloride (0.523 g, 5.36 mmol, 1.2 eq) and stirred at 0°C. Methyl magnesium bromide (18.42 mL, 18.41 mmol, 4.5 eq) was then added dropwise and the reaction was allowed to stir. The reaction was heated to room temperature and was allowed to stir until complete conversion to ketone was observed by LCMS. The reaction mixture was quenched with a solution of saturated NH₄Cl slowly and allowed to stir for 10 minutes, then basified with 10% NaOH dropwise. The mixture was further partitioned with EtOAc and separated. The aqueous

layer was extracted with EtOAc once more and then DCM twice. The organic layers were combined, dried over anhydrous sodium sulfate, filtered, and concentrated to afford 1-(1-((3-chloropyridin-4-yl) methyl) piperidin-4-yl)ethanone (1.2g, 100% yield). LCMS 75-95% 3 minutes MeOH:H₂O gradient >95% pure rt = 0.644 min. LCMS 50-95% 8 minutes MeOH:H₂O gradient >95% pure rt = 0.745 min. HRMS calc'd for C₁₃H₁₈ClN₂O 253.1108; found [M+H] 253.1100.

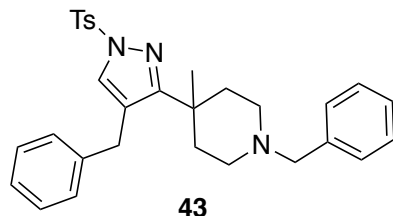


1-benzyl-4-methylpiperidine-4-carbaldehyde (34). In a flame dried flask was added 8 mL dry DCM and DMSO (0.972 mL, 13.7 mmol, 3 eq) and cooled to -78 °C. To the solution was added 2 M oxalyl chloride (0.878 mL, 10.0 mmol, 2.2 eq) dropwise. Solution was stirred for 30 minutes. A solution of (1-benzyl-4-methylpiperidin-4-yl)methanol (1.0 g, 4.55 mmol) in 5 mL Dry DCM was then added to the "swern" flask. The solution was allowed to stir for 30 minutes. Then TEA (2.54 mL, 18.24 mmol, 4 eq) was added dropwise. Reaction was then allowed to warm to RT. After two hours, reaction was quenched with diethyl ether. Then the organic layer was washed with ammonium chloride, then sodium bicarbonate, then brine. The organic was dried over anhydrous magnesium sulfate, filtered, and concentrated to afford 1-benzyl-4-methylpiperidine-4-carbaldehyde (646 mg, 65% yield). LCMS 50-95% 3 minutes MeOH:H₂O gradient >95% pure rt = 0.608 min. LCMS 75-95% 3 minutes MeOH:H₂O gradient >95% pure rt = 0.519 min. HRMS calc'd for C₁₄H₂₀NO 218.1545; found [M+H] 218.1537.



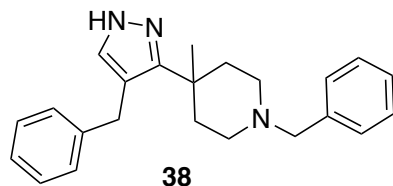
(E)-N'-((1-benzyl-4-methylpiperidin-4-yl)methylene)-4-methyl-N-(prop-2-yn-1-yl)benzenesulfonohydrazide (42). 1-benzyl-4-methylpiperidine-4-carbaldehyde (750 mg, 3.45 mmol) was dissolved in 10 mL MeOH and heated to 60°C. Toluenesulfonohydrazide (642 mg, 3.45 mmol) was added and reaction was allowed to stir for 2 hrs. The reaction was taken off heat, and solvent was removed under vacuum to afford tosylhydrozone intermediate which was taken to the next reaction. (E)-N'-((1-benzyl-4-methylpiperidin-4-yl)methylene)-4-methylbenzenesulfonohydrazide (434 mg, 1.25 mmol) and propargyl bromide (1.25 mmol, 1.1 eq) were dissolved in 20 mL dry DMF. K₂CO₃ (1.2526 mmol, 1.1 eq) was added and the reaction was stirred at room temperature for 2 hrs. Upon completion H₂O (20 mL x 3) was added, extracted with EtOAc (20 mL), and the organic layers were combined and dried over magnesium sulfate. The solvent was removed under vacuum, and the residue was further purified by silica gel column chromatography to afford (E)-N'-((1-benzyl-4-methylpiperidin-4-yl)methylene)-4-methyl-N-(prop-2-yn-1-yl)benzenesulfonohydrazide (380 mg, 78% yield over 2

steps). LCMS 50-95% 6 minutes MeOH:H₂O gradient >95% pure rt = 1.69 min. LCMS 75-95% 6 minutes MeOH:H₂O gradient >95% pure rt = 0.579 min.

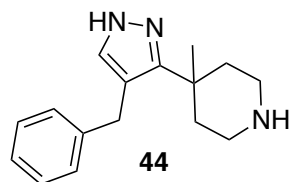


1-benzyl-4-(4-benzyl-1-tosyl-1H-pyrazol-3-yl)-4-methylpiperidine (43). In a flame dried flask, (*E*)-*N'*-((1-benzyl-4-methylpiperidin-4-yl)methylene)-4-methyl-*N*-(prop-2-yn-1-yl)benzenesulfonohydrazide (360 mg, 0.850 mmol) and iodobenzene (94.7 μ l, 0.850 mmol, 1 eq) were dissolved in dry DMF and degassed for 20 minutes.

bis(triphenylphosphine)palladium(II) chloride (29.8 mg, 0.0425 mmol, 0.05 eq) was added followed by CuI (8.09 mg, 0.0425 mmol, 0.05 eq). After 5 minutes, degassed TEA (3.6 mL, 25.79 mmol, 30 eq) was added. The reaction was stirred at 80°C for 1 hour. Upon completion, H₂O was added and extracted with EtOAc (3 times). Organic layers were combined, dried over magnesium sulfate, and concentrated to afford 1-benzyl-4-(4-benzyl-1-tosyl-1H-pyrazol-3-yl)-4-methylpiperidine (340 mg, 80% yield). LCMS 50-95% 6 minutes MeOH:H₂O gradient >95% pure rt = 0.595 min. LCMS 75-95% 3 minutes MeOH:H₂O gradient >95% pure rt = 0.785 min.

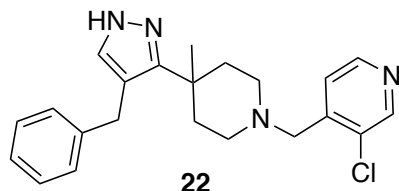


1-benzyl-4-(4-benzyl-1H-pyrazol-3-yl)-4-methylpiperidine (38). The tosyl-protected precursor **43** was dissolved in DMF and potassium tert-butoxide was added. Reaction was allowed to run overnight. Upon completion, brine was added and the aqueous layer was extracted with EtOAc (3 times). The organic layers were combined, dried over magnesium sulfate, and concentrated to afford 1-benzyl-4-(4-benzyl-1H-pyrazol-3-yl)-4-methylpiperidine. Product was moved to the next step without further purification.



4-(4-benzyl-1H-pyrazol-3-yl)piperidine (44). To a solution of **38** in *t*-BuOH (0.1 M) and AcOH (0.01 M) was added Pd/C (10-50% by mass). The reaction was hydrogenated under an atmosphere of H₂ between 45-55 psi on a parr hydrogenator overnight. Once the reaction was

completed, the H₂ gas was purged and the reaction vessel was flushed with argon. The crude reaction mixture was filtered through two fluted pieces of filter paper and concentrated *in vacuo*. The mixture was then diluted with brine and DCM followed by basification with 10% NaOH. The layers are separated and the aqueous layer extracted with DCM (3 times). The organic layers are combined, dried over anhydrous sodium sulfate, filtered and concentrated to afford the crude product which if necessary was purified by column chromatography.



4-((4-(4-benzyl-1H-pyrazol-3-yl)-4-methylpiperidin-1-yl)methyl)-3-chloropyridine (**22**). To a solution of the 4-(4-benzyl-1H-pyrazol-3-yl)-4-methylpiperidine (18.0 mg, 0.071 mmol) in DCM (0.1 M) was added the aldehyde (1.1 eq) and stirred at room temperature for 15 minutes. A drop of acetic acid was added and the reaction was allowed to stir for 15 minutes. Sodium triacetoxyborohydride (1.5 eq) was added as one portion to the reaction. The reaction was complete after 5 hrs. Upon completion the mixture was diluted with brine and basified with 1 M NaOH. The layers are separated and the aqueous layer extracted with DCM (3 times). The organic layers were combined, dried over anhydrous sodium sulfate, filtered and concentrated to afford the crude product 4-((4-(4-benzyl-1H-pyrazol-3-yl)-4-methylpiperidin-1-yl)methyl)-3-chloropyridine. The crude product was pure without further purification.

References

1. UNAIDS. The Global HIV/AIDS Epidemic. (<https://www.hiv.gov/hiv-basics/overview/data-and-trends/global-statistics>); 2016. Accessed 21 March 2018.
2. Centers for Disease Control and Prevention (CDC) Fact Sheet. Today's HIV/AIDS Epidemic. (<https://www.cdc.gov/nchstp/newsroom/docs/factsheets/todaysepidemic-508.pdf>); 2016. Accessed 21 March 2018.
3. World Health Organization. Antiretroviral Therapy. (http://www.who.int/topics/antiretroviral_therapy/en/); 2016. Accessed 26 March 2018.
4. Fauci, A. S.; Folkers, G. K.; Dieffenbach, C. W., HIV-AIDS: much accomplished, much to do. *Nat. Immunol.* **2013**, *14* (11), 1104-7.
5. Este, J. A.; Telenti, A., HIV entry inhibitors. *Lancet* **2007**, *370* (9581), 81-8.
6. Henrich, T. J.; Kuritzkes, D. R., HIV-1 entry inhibitors: recent development and clinical use. *Curr. Opin. Virol.* **2013**, *3* (1), 51-7.
7. De Clercq, E., The bicyclam AMD3100 story. *Nat. Rev. Drug Discov.* **2003**, *2* (7), 581-7.
8. Briz, V.; Poveda, E.; Soriano, V., HIV entry inhibitors: mechanisms of action and resistance pathways. *J Antimicrob. Chemother.* **2006**, *57* (4), 619-27.
9. Fatkenheuer, G.; Nelson, M.; Lazzarin, A.; Konourina, I.; Hoepelman, A. I.; Lampiris, H.; Hirschel, B.; Tebas, P.; Raffi, F.; Trottier, B.; Bellos, N.; Saag, M.; Cooper, D. A.; Westby, M.; Tawadrous, M.; Sullivan, J. F.; Ridgway, C.; Dunne, M. W.; Felstead, S.; Mayer, H.; van der Ryst, E.; Motivate; Teams, M. S., Subgroup analyses of maraviroc in previously treated R5 HIV-1 infection. *N. Engl. J. Med.* **2008**, *359* (14), 1442-55.
10. Moyle, G.; DeJesus, E.; Boffito, M.; Wong, R. S.; Gibney, C.; Badel, K.; MacFarland, R.; Calandra, G.; Bridger, G.; Becker, S.; Team, X. A. C. T. S., Proof of activity with AMD11070, an orally bioavailable inhibitor of CXCR4-tropic HIV type 1. *Clin. Infect. Dis.* **2009**, *48* (6), 798-805.
11. Wolfe, A. D.; Rush, R. S.; Doctor, B. P.; Koplovitz, I.; Jones, D., Acetylcholinesterase prophylaxis against organophosphate toxicity. *Fundam. Appl. Toxicol.* **1987**, *9* (2), 266-70.
12. Cox, B. D.; Prosser, A. R.; Sun, Y.; Li, Z.; Lee, S.; Huang, M. B.; Bond, V. C.; Snyder, J. P.; Krystal, M.; Wilson, L. J., Pyrazolo-piperidines exhibit dual inhibition of CCR5/CXCR4 HIV entry and reverse transcriptase. *ACS Med. Chem. Lett.* **2015**, *6* (7), 753-7.
13. Prosser, A. R.; Liotta, D. C., One-pot transformation of esters to analytically pure ketones: Methodology and application in process development. *Tetrahedron Lett.* **2015**, *56* (23), 3005-7.
14. Viegas, A.; Manso, J.; Nobrega, F. L.; Cabrita, E. J., Saturation-transfer difference (STD) NMR: a simple and fast method for ligand screening and characterization of protein binding. *J. Chem. Ed.* **2011**, *88* (7), 990-4.

15. Yang, Y.; Hu, Z.-L.; Li, R.-H.; Chen, Y.-H.; Zhan, Z.-P., Pyrazole synthesis via a cascade Sonogashira coupling/cyclization of N-propargyl sulfonylhydrazones. *Org. Biomol. Chem.* **2018**, *16* (2), 197-201.